MASTER THESIS

Trace element analysis based on neutron activation with coincident gamma ray detection

Jessica Delgado

August 9, 2017

LUND UNIVERSITY

Supervisor: Linus Ros

Co-supervisor: Per Kristiansson

Department of Physics

Division of Nuclear physics

Lund University

Abstract

In this work, six soil samples have been analyzed. The samples come from different sedimentary layers on Earth. They were previously studied with the objective to find the trace concentration of iridium, to correlate the increased concentrations of iridium with meteorite impacts that have occurred to the Earth. In this work the samples are reanalyzed with the purpose to investigate which other trace elements can be detected.

Before the measurement with the gamma spectrometer, the samples are activated in a thermal neutron reactor. The radiation from the samples is detected with a setup that consists of 14 $LaBr_3$:Ce detectors. The gamma rays from the different elements in the sample should be well separated, but this is not always possible. There is a background coming from the Compton scattering effect, which causes problems in the spectra and causes difficulties in the quantification of trace elements. To improve the sensitivity of the spectrometer and reduce background, a coincidence condition on two or more gamma rays can be applied. The condition is characteristic for each element.

Using this technique, the identification of 7 different isotopes in the previous measured samples (^{46}Sc, ^{134}Cs, ^{60}Co, ^{58}Co, ^{124}Sb, ^{181}Hf and ^{152}Eu) was possible. Additionally, the amounts of each element in the samples were estimated by comparing with the previous data. The amounts obtained were in the order of ppm. The minimum concentration needed in order to assure the presence of the element in the sample was calculated for each isotope and a limit below 1 ppm was obtained for all the elements. This means that by using the coincidence gamma ray spectrometer it was possible to identify low concentration of elements in the samples.

Acknowledgments

First, I want to thank my supervisor Linus Ros for guiding me during the whole project. For always being available for me, answering my questions and doubts, and for giving me the necessary bases for the development of the project.

I want to thank my co-supervisor Per Kristiansson for giving me the opportunity to do my thesis at Lund University, that is an honor and a privilege for me. I also would like to thank Charlotta Nilsson for correcting my thesis, giving me constructive and necessary corrections.

To Natasa Lalovic and Christian Lorenz who took part of their time in giving me good corrections on my thesis, despite they were busy on their work trip. Thanks to my colleges Amanda Jalgen and Nicholai Mauritzson with whom I shared the office during the project. Especially I would like to thank Nicholai Mauritzson for always being so helpful, and advise me when I needed it.

I cannot forget to thank Jose Ignacio Carreño, who has welcomed me to Lund and giving me his help. To Nathaly de la Rosa for always offer me her help. To my dear friends who supported me during the process Luisana Duque and Zafer Demirtas.

Last but not least, I want to thank my beautiful family. Thank mom and dad for giving me the opportunity to do my thesis here. I am able to do this thanks to all the effort you have done for me. Also I would like to say thanks to my lovely brother and sister, Jonathan and Jennifer for always supporting me in everything and giving me so much love.

List of Figures

1 Compton Scattering Scheme 5
2 Decay Scheme of ^{46}Sc 9
3 Energy band structure of an activated crystalline scintillator 10
4 Overview of the coincidence spectrometer, at the LIBAF. 14
5 Setup consisting of the 14 $LaBr_3$:Ce detectors 15
6 Setup consisting of the 14 $LaBr_3$:Ce detectors plus 6 plastic scintillators 15
7 Scheme of the electronic setup for two of the 14 detectors. 16
8 Decay scheme of ^{58}Co 21
9 Time difference of coincidence vs counts. 22
10 Energy spectrum of ^{46}Sc 26
11 Energy spectrum of ^{58}Co 26
12 Energy spectrum of ^{60}Co 27
13 Energy spectrum of ^{124}Sb 27
14 Energy spectrum of ^{134}Cs 27
15 Energy spectrum of ^{152}Eu 27
16 Energy spectrum of ^{181}Hf 27

List of Tables

1 Elemental concentration. 17
2 Capture cross section and abundance of the isotopes 18
3 Gamma rays energies per element used for identification, applying double or triple coincidence conditions 19
4 Samples mass 22
5 Compensated counts of every isotope in the samples. 24
6 Estimation calculated of the isotopes concentration. 25
7 Minimum Detectable Limit for the sample 8. 26

List of Abbreviations

CFD	Constant Fraction Discriminator
DAQ	Data acquisition
GG	Gate Generator
HPGe	High Purity Germanium detector
$LaBr_3$:Ce	Cerium-doped Lanthanum Bromide
LIBAF	Lund Ion Beam Analysis Facility
MDA	Minimum Detectable Activity
MDL	Minimum Detectable Limit
NAA	Neutron Activation Analysis
NIM	Nuclear Instrumentation Module
PPB	Part Per Billion
PPM	Part Per Million
QDC	Charge to Digital Converter
TDC	Time to Digital Converter

Contents

1 Introduction **1**

2 Interaction of gamma rays with matter **4**

2.1 Photoelectric Effect. 4

2.2 Compton Scattering Effect 4

2.3 Pair Production 5

3 Radioactive Decay **6**

3.1 Alpha Decay 6

3.2 Beta Decay 6

3.3 Gamma Decay 7

3.4 Electron Capture 7

4 Coincidence Technique and Neutron Activation Analysis **8**

4.1 Neutron Activation Analysis (NAA) 8

4.2 Basic Coincidence gamma ray Technique 8

5 Scintillation Detectors **10**

5.1 Lanthanum-Bromide $LaBr_3$:Ce Detector 10

5.2 Photomultiplier 11

6 Electronic Devices **12**

6.1 Nuclear Instrumentation Module (NIM) 12

6.2 Constant Fraction Discriminator (CFD) 12

6.3 Charge to Digital Converter (QDC) 12

6.4 Time to Digital Converter (TDC) 13

6.5 Scaler 13

6.6 Gate Generator (GG) 13

6.7 MCFD-16 13

6.8 Software Kmax 13

7 Experimental Setup **14**

7.1 Overview 14

7.2 Electronic Setup 15

8 Experimental Methodology **17**

8.1 Isotopes Selection 17

8.2 Gamma ray selection 18

8.3 Elements measured 19

8.3.1 Condition applied to measure ^{181}Hf. 20

8.3.2 Condition applied to measure ^{58}Co. 20

8.3.3 Condition applied to measure ^{152}Eu. 21

8.4 Compensation and normalization of the counts 22

8.5 Minimum Detectable Limit calculation 23

9 Results and Discussion **24**

9.1 Results 24

9.2 Discussion 28

10 References **30**

Chapter 1

1 Introduction

The history of nuclear physics started at the end of the 19th century in 1896, when the French physicist Antoine Henri Becquerel discovered the radioactivity, a phenomenon which describes the characteristic of a material to emit radiation [1]. The emission of radiation is a feature of many atoms, where the number of neutrons in the nuclei is too low or excessive, which leads to instability. To reach a stable configuration, the nucleus releases energy in the form of radiation. The nuclei have different ways of disintegration, but there are three principle ways: alpha decay, where the nuclei emit one alpha particle (a Helium nucleus), beta decay, which means the emission of a beta particle (an electron or positron) and finally by gamma radiation, where the excess energy is released in form of a photon [2].

After the discovery of radiation, different techniques have been developed in order to study and identify the sources of radiation and its properties. One example is the development of the first scintillation device capable of detecting radiation, by William Crookes in 1903 [3]. Scintillation detectors are today one of the most important and most used detectors for gamma ray spectrometry. They have a high efficiency and a good resolution, which provide a positive linear conversion between the radiation energy deposited in the detector and the electric signal of the detector [2].

In order to identify a specific element, the gamma rays from one element should be well separated from the gamma rays of the other elements in the samples. Unfortunately this is not always possible. The background sometimes can severely affect a spectrum. The background can be caused by the Compton scattering effect, where a gamma ray from the radioactive sample interacts with an electron, and then a scattered gamma is created with lower energy. The detector also detects this unwanted scattered photon, and this obstructs the quantification of the trace elements [2].

One way to reduce this effect is by applying the Coincidence Technique. The coincidence technique was established in 1924 by Hans Geiger and Walther Bothe. They used the technique, when they wanted to measure the simultaneous occurrence of the scattered photon and the recoil electron in the Compton scattering effect. Later in 1930 they improved the technique with the invention of the first electronic coincidence circuit [4]. With the innovation of

advanced and high efficiency detectors, the coincidence technique became one of the most important tools in nuclear and particle physics research, because it represents a strong criterion for distinguishing reactions [2].

The method behind the coincidence gamma ray spectrometer is a non-destructive technique, which does not require the chemical dissolution of the material [5]. It consists of two or more detectors working in coincidence mode. This method can only be applied to samples that are radioactive. A sample can become radioactive by irradiating the sample with thermal neutrons during a period of time. The nuclei of the samples can absorb the neutrons, so the ratio of neutrons and protons changes, making the nuclei unstable. Therefore, they will decay by one of the previously mentioned decays and emit radiation until they are stable [6].

The combination of the multi-gamma rays detection in coincidence mode and the neutron activation represents a good trace element quantification technique, with a high sensitivity. Furthermore, it is possible to simultaneously analyze the sample for several elements [5]. Therefore, in this work the combination of both techniques was applied to six ash samples in order to identify the trace elements in these samples. The coincidence spectrometer used is a setup of 14 $LaBr_3$:Ce scintillation detectors, arranged around the sample.

The six ash samples investigated belong to different sedimentary layers, which were previously examined by Birger Schmitz and coworkers at Lund University with the purpose to identify the iridium concentration [7, 8]. The interest in measuring iridium concentration is due to the fact that iridium is an indicator for impacts of meteorites to the Earth. The Earth itself has just very small concentrations of iridium, but in the rest of the solar system the amount of iridium is comparably high. Therefore the detection of iridium and the measurement of its concentration is a very good tool to locate where and when meteorites impacted on earth. The only method capable of measuring traces of iridium is the combination of NAA and the coincidence technique [7, 8].

Three of the samples are volcanic ash layers, collected from the Fur Formation of Early Eocene age in Denmark [7]. The other three ash samples are from fossil meteorites found in the Orthoceratite Limestone at Kinnekulle, in southern of Sweden. During the previous studies of the samples, besides measuring the concentration of iridium, also other traces elements were measured, as: Sc, Ni, Cs, Co, Se, Sb, Ta, Hf and Th [8].

The purpose of this work is to reanalyze six ash samples by the use of the 14 $LaBr_3$:Ce coincidence spectrometer located at the LIBAF (Lund Ion Beam Analysis Facility in Sweden), with the objective to identify and measure the trace elements present in the samples. Before doing the analysis some theoretical studies have to be conducted. First, it has to be selected which isotopes from the elements can be measured, taking into consideration that the samples have to be activated with thermal neutrons before the experiment. An isotope means an element with the same proton numbers but different neutron number. Second, every isotope decays in a different way, so it must be found a suitable combination of gamma ray coincidence, by studying the decay scheme of every isotope.

Chapter 2

2 Interaction of gamma rays with matter

The detection of gamma rays is based on the interaction between the radiation emitted from a radioactive source and the detector material. The probability of interaction between a photon and the detector material depends on the incident photon energy and the atomic number Z of the material. The three main interactions between matter and radiation are: photoelectric effect, Compton scattering effect and pair production. In all these processes a photon transfers all or part of its energy to an electron [2].

2.1 Photoelectric Effect.

The photoelectric effect is a phenomenon where an incident photon interacts with a bound electron. The electron completely absorbs the energy from the photon, and it is ejected from its orbit. The energy of the electron is equal to:

$$E_e = h\nu - E_b \tag{1}$$

where E_b is the binding energy of the electron, $h\nu$ is the photon energy and E_e is the kinetic energy of the escaping electron [2].

2.2 Compton Scattering Effect

The Compton Effect occurs when a photon collides with a free electron located in a material. The photon is scattered with a θ angle (see **Figure 1**). The wavelength of the photon increases, hence the photon energy decreases and it is equal to:

$$h\nu' = \frac{h\nu}{1 + \frac{h\nu}{m_0 c^2}(1 - cos\theta)} \tag{2}$$

where $h\nu$ represents the original energy of the photon, $h\nu'$ the new energy of the scattered photon and m_0c^2 the energy of the electron before the interaction [2].

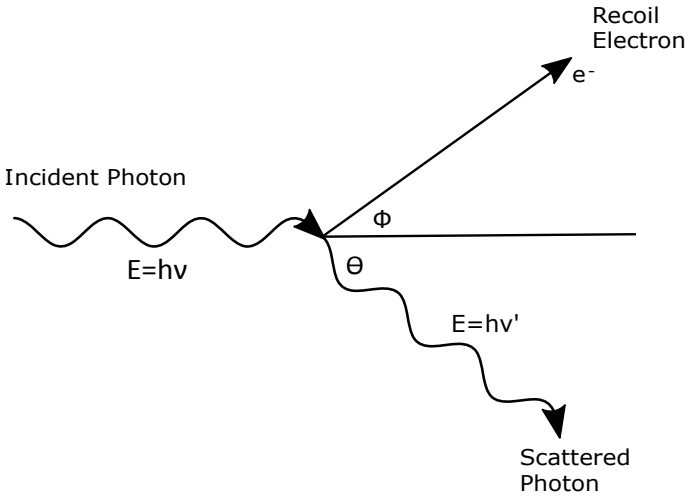

Figure 1: Compton Scattering Scheme. Figure adapted from: [2]

2.3 Pair Production

The pair production process occurs the following way: a photon in an electric field, e.g. from nucleus, disintegrates into two particles, a positron e^+ and an electron e^-. This phenomenon only occurs if the photon energy is higher than 1.02 MeV. After the pair production occurs, the positron slows down as it travels through the material and eventually annihilates with an electron. In this annihilation process two photons with 511 keV energies are created with opposite directions [2].

Chapter 3

3 Radioactive Decay

The atomic nuclei are built of protons and neutrons. Some nuclei have a stable configuration but there are others that are unstable, hence they release energy until they reach a stable configuration [1]. There are many ways the nuclei release the energy, by emitting particles or gamma rays. The most important radioactive decays are:

3.1 Alpha Decay

It is a process where a nucleus has to reduce its mass in order to achieve a nuclear stability. The nucleus decays by emitting an alpha particle, which contains two protons and two neutrons. The atomic number of the remaining nucleus is lowered by two and its mass number lowered by four compared to the initial nucleus [1].

$$ {}^{A}_{Z}X \rightarrow {}^{A-4}_{Z-2}Y + {}^{4}_{2}\alpha \tag{3} $$

3.2 Beta Decay

Beta decay is a process where an unstable nucleus becomes stable by emitting a beta particle, to improve the neutron to proton ratio of the nucleus. There are two types of beta decay:

- β^- decay: a process where a neutron decays into a proton, an electron and an electron anti neutrino [1]:

$$ {}^{A}_{Z}X \rightarrow {}^{A}_{Z+1}Y + \beta^- + \bar{\nu_e} \tag{4} $$

- β^+ decay: a process where a proton decays into a neutron, a positron and an electron neutrino [1]:

$$ {}^{A}_{Z}X \rightarrow {}^{A}_{Z-1}Y + \beta^+ + \nu_e \tag{5} $$

In the β^+ decay the annihilation process occurs as in the Pair Production, explained previously in **Chapter 2**. The positron travels through the medium and collides with an electron, both particle are annihilated and two photons with 511 keV energies are created with opposite directions [1].

3.3 Gamma Decay

The gamma decay is a process where a nucleus is in an excited state and releases this excess energy by emitting a gamma ray. The proton and neutron numbers of the nucleus are not changed during the process [1].

$$ {}^{A}_{Z}X \rightarrow {}^{A}_{Z}Y + \gamma \tag{6} $$

3.4 Electron Capture

It is a process where a proton 'captures' an electron and forms a neutron and an electron neutrino. The electron originated mostly from one of the inner shells of the atom [1].

$$ p + e^{-} \rightarrow n + \nu_{e} \tag{7} $$

Chapter 4

4 Coincidence Technique and Neutron Activation Analysis

Two important techniques are applied in this work, in order to measure the trace elements of the six ash samples. Their underlying principles are described in this Chapter.

4.1 Neutron Activation Analysis (NAA)

The Neutron Activation Analysis (NAA) is a non-destructive, highly sensitive method for the detection of traces in different materials. The principle of NAA is the following: the sample is irradiated with neutrons and occasionally a nucleus in the sample absorbs one neutron, the nucleus becomes unstable and decays. The daughter nucleus sometimes ends up in an excited state and releases the energy by sending out one or several gamma rays. By analyzing the radiation from the sample it is possible to distinguish the elements in the sample. This is possible because the energy of every gamma ray is characteristic of a particular chemical element, and the number of gamma rays detected is proportional to the amount of the specific element in the sample [5].

4.2 Basic Coincidence gamma ray Technique

Coincident gamma ray detection means the detection of two gamma rays or more, which are emitted almost simultaneously or within a very short time, from the decay of a radioactive nucleus. This gamma ray cascade is produced by an excited nucleus that releases its energy by going from one excited state to another with less energy, where a gamma ray is produced. It stays in that state for a short period of time and later it decays again to another lower state releasing another gamma ray [2]. This process is explained by **Figure 2**, it shows the decay of ^{46}Sc, where two gamma rays are emitted in coincidence. ^{46}Sc decays by beta decay to the second excited state, then it de-excites from the second to the first excited state by releasing the first gamma ray. It stays there for 0.0051 ns and finally it reaches stable configuration (its ground state) after emitting the second gamma ray with an energy equal to 889 keV. In a measurement using the coincidence technique, both gamma rays are detected. Since two gamma rays are detected, it is called a double coincidence.

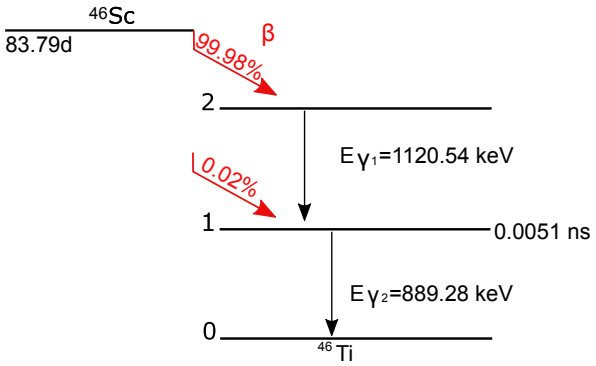

Figure 2: Decay Scheme of ^{46}Sc. Figure adapted from: [9]

To identify elements using a combination of NAA and the coincidence technique several steps have to be conducted. First one has to identify which isotope from a certain element has a good neutron capture cross section. Second for each isotope one should note which gamma rays could be observed in coincidence. The intensity and energy of the gamma rays of interest should be noted. In the text, double and triple coincidence terms refer to cases when two and three gamma rays are measured in coincidence, respectively.

Chapter 5

5 Scintillation Detectors

A scintillator is a material that exhibits luminescence, when ionizing radiation passes through it. The main purpose of a detector is to make a linear and proportional conversion, between the energy deposited in the detector and the voltage output of the detector. There are two types of scintillators: organic scintillators that are more used to detect charged particles and inorganic scintillators that are more convenient for gamma rays detection because it has a higher atomic number. Consequently, the electron density of the material is higher, leading to a higher efficiency for detecting photons [2].

The mechanism of an inorganic scintillator crystal can be explained in terms of electronic bands of the material, see **Figure 3**. The electric structure of a crystal consists of discrete energy levels, called bands. In the ground state, the valence band is generally filled and the conduction band is empty. Incident radiation can excite an electron from the valence band to the conduction band. At some point, this electron will lose its energy, emitting a photon and falling back into the valence band. This photon is the one that will be collected by the photomultiplier. To increase the probability of photon emission, the crystals are doped with impurities, called activators. Thereby, additional energy states in the band gap between the valence and the conduction band are created, giving the electrons more energy states to excite and de-excite to [2].

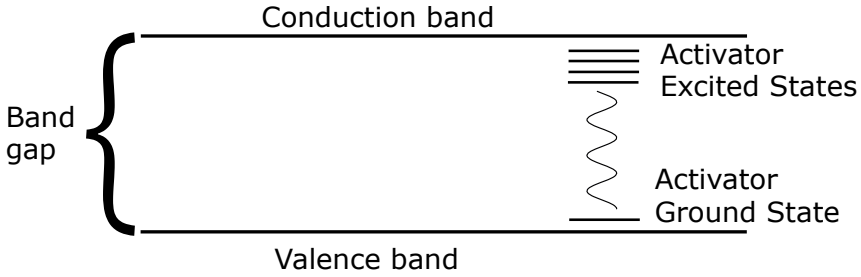

Figure 3: Energy band structure of an activated crystalline scintillator. Figure adapted from: [2]

5.1 Lanthanum-Bromide $LaBr_3$:Ce Detector

The Lanthanum Bromide detectors are inorganic scintillation detectors that became famous in the past years, for gamma ray spectroscopic research, thanks to its high resolution and

good linear response. The crystal of the detector is doped with an activator of 0.5% cerium, to improve the light output. It has a timing resolution of 260 ps for 0.5% of cerium, an energy resolution of 3% at 662 keV, a light output of 60000 photons/MeV [11]. Therefore, with this high light emission the photomultiplier can have less dynodes, leading to an improved time resolution. It has a good linearity response for energy higher than 60 keV. The timing property of the detector strongly depends on the cerium concentration. The decay time constant decreases when the cerium amount increases. The decay time constant hardly varies between different temperatures, so it does not need cooling [11, 12].

Despite the High Purity Germanium detectors (HPGe) have the best energy resolution (0.2% at 1 MeV), the inorganic scintillators also have many applications in gamma ray spectroscopy, thanks to their high atomic number that gives a better intrinsic efficiency and also they are much easier to maintain than HPGe detectors. Additionally, the inorganic scintillators, such as the $LaBr_3$:Ce detectors, have a good timing resolution, therefore it represents an appropriate and qualified device for the application of the coincidence technique [12].

5.2 Photomultiplier

A scintillation detector is usually coupled to a photomultiplier, to transform the light from the scintillation crystal into an electrical signal. A photomultiplier consists of a photocathode where photoelectrons are created by the photoelectric effect when the scintillation light is hitting the cathode. These photoelectrons are accelerated to the first dynode, by a voltage difference. The accelerated photoelectrons impact on the dynode causing the emission of several additional electrons. These are accelerated again to the next dynode, and so on. The current produced is collected at the anode, and can be amplified and recorded [10].

Chapter 6

6 Electronic Devices

This chapter describes the electronic instruments, which were used in order to process the signal detected from the 14 $LaBr_3$:Ce detectors.

After detecting the radiation, the detector provides an electrical signal as a result, and an electronic system is needed to process that signal. Every electronic device has a different function, e.g. obtaining the energy information, processing a delay, changing the shape of the signal, converting analog signal into digital or even determining the time between two signals, etc. An analog signal carries the amplitude of the signal whereas the digital signal carries the information coded in binary logic, represented by two states, 1 or 0 [10].

6.1 Nuclear Instrumentation Module (NIM)

The NIM (Nuclear Instrumentation Module) is a standard for electronic modules used in nuclear and particle physics. All electronic devices of an experiment are located and organized in a modular form, following the NIM standard [10].

6.2 Constant Fraction Discriminator (CFD)

A constant fraction discriminator is an electronic device that discriminate the signal. It processes the analog signal, and it gives a digital output as a result if the input signal reaches a threshold level determined [2].

6.3 Charge to Digital Converter (QDC)

The Charge to Digital Converter is a device that converts the charge pulse into a digital number. This process occurs by charging a capacitor with the input charge signal. While the capacitor is being discharged at a constant rate, a scaler counts the pulses, with a clock with a known frequency. The counts counted by the scaler are equal to the charge of the capacitor, thus proportional to the charge input pulse [10]. In this project the QDC used is the CAEN QDC model V792N. The module houses 16 input channels [13].

6.4 Time to Digital Converter (TDC)

The Time to Digital Converter is an electronic device that processes the time of an event, and as result it gives a digital signal of the time information. In the present work the TDC used is the CAEN V1290N TDC model. The module has 16 input channels and one output common to every channel [14].

6.5 Scaler

It is an unit that is in charge of counting the number of pulses from an input signal and this information can be shown on a display embedded in the unit or it is read on a computer [10].

6.6 Gate Generator (GG)

Using this unit, a gate for the data acquisition is set. A specific delay and width of the gate can be specified [10].

6.7 MCFD-16

This is an electronic device that works as a discriminator with 16 channels. It contains a fast pre-amplifier, a CFD and a Pattern Proceeding unit, which has a coincidence window that can be set between 5 ns and 600 ns [15].

6.8 Software Kmax

Kmax is a software system made for data acquisition and analysis. It contains a wide range of applications like: graphical user-interface elements, a broad base for modular instrumentation, a java application which enables the user to add elements or modify the analysis method, etc [16]. The data of this project is analyzed using this software.

Chapter 7

7 Experimental Setup

The coincident gamma rays can be observed by using a setup of two or more detectors, in order to detect the double or triple coincidences. The signal detected travels through an electronic setup, which converts the input signal into a logical signal and then the result is sent to a coincidence window. This window is 'in charge' of deciding if the two signals are in coincidence and if the requirement is fulfilled, a logical signal is produced as an output. Otherwise the signal is rejected [10].

7.1 Overview

The experiment presented in this work was carried out in November 2016 using the coincidence gamma ray spectrometer located at LIBAF (Lund Ion Beam Analysis Facility in Sweden).

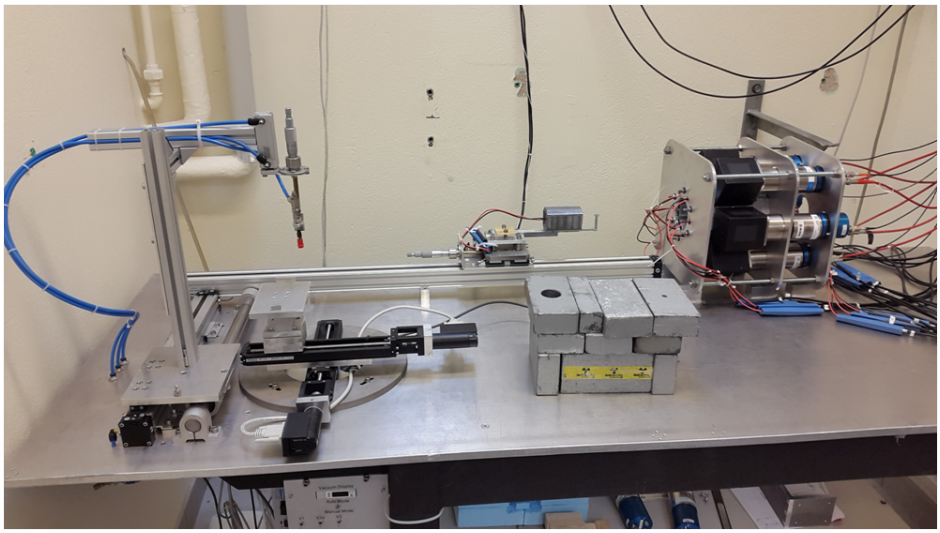

Figure 4: Overview of the coincidence spectrometer, at the LIBAF.

Figure 4 shows the coincidence spectrometer at the LIBAF. To the right of the figure there are 14 $LaBr_3$:Ce detectors, each coupled to a photomultiplier. Twelve of the detectors are cylindrically distributed around the source, and two are located at both ends of the cylinder, **Figure 5** shows the distribution. The cylindrical detector arrangement is surrounded by 6 plastic scintillators, responsible for capturing those gamma rays that were not absorbed by the $LaBr_3$:Ce detectors and it is used as a Compton suppression shield. The arrangement

of the plastic scintillators is shown in **Figure 6**. While the samples are not being used, they are placed inside an arrangement of lead blocks shown in **Figure 4**. The lead blocks serve as a radiation shield. When a sample should be analyzed, it is inserted into the cylindrical detector arrangement by an automatic hand. Every source is sealed inside a glass ampoule.

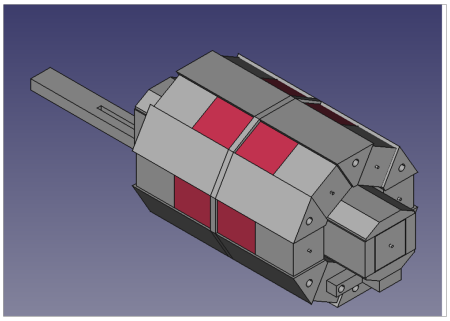

Figure 5: Setup consisting of the 14 $LaBr_3$:Ce detectors. Figure courtesy of Linus Ros.

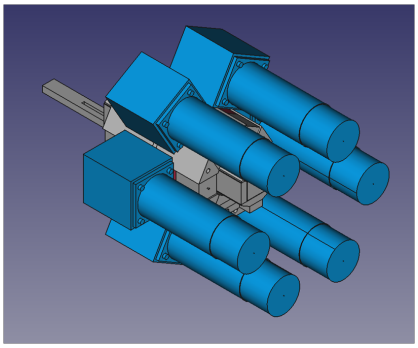

Figure 6: Setup consisting of the 14 $LaBr_3$:Ce detectors plus 6 plastic scintillators. Figure courtesy of Linus Ros.

7.2 Electronic Setup

The signal from the 14 detectors, after passing through the photomultiplier, is sent to the MCFD-16 device. In the MCFD-16 the signal is discriminated by the CFD, with values higher than 60 keV. The MCFD-16 generates a trigger if two or more signals enter into the device, within a window of 50 ns.

After this the time signal is sent to a TDC. At this stage the time between the coincidence pulses is counted and transformed into a digital signal (see **Figure 7**, the red lines). Energy signals are sent to a QDC, where the signal is integrated and transformed into a number (see the yellow lines in **Figure 7**). The TDC and the QDC represent the data acquisition.

At the same time the GG receives the signal directly from the MCFD16, and upon receiving the signal, it opens the gate for data acquisition (DAQ). The DAQ Veto is in charge of notifying the GG if the data acquisition is busy or not. If the data acquisition is busy the GG does not trigger. In case it is not busy, the GG triggers and sends a signal to the scaler and to the DAQ. The scaler receives the gate signal from the GG and the triggered signal from the MCFD16, and it counts them. These values are later used to compensate the data for the live time of the system (see **Figure 7**).

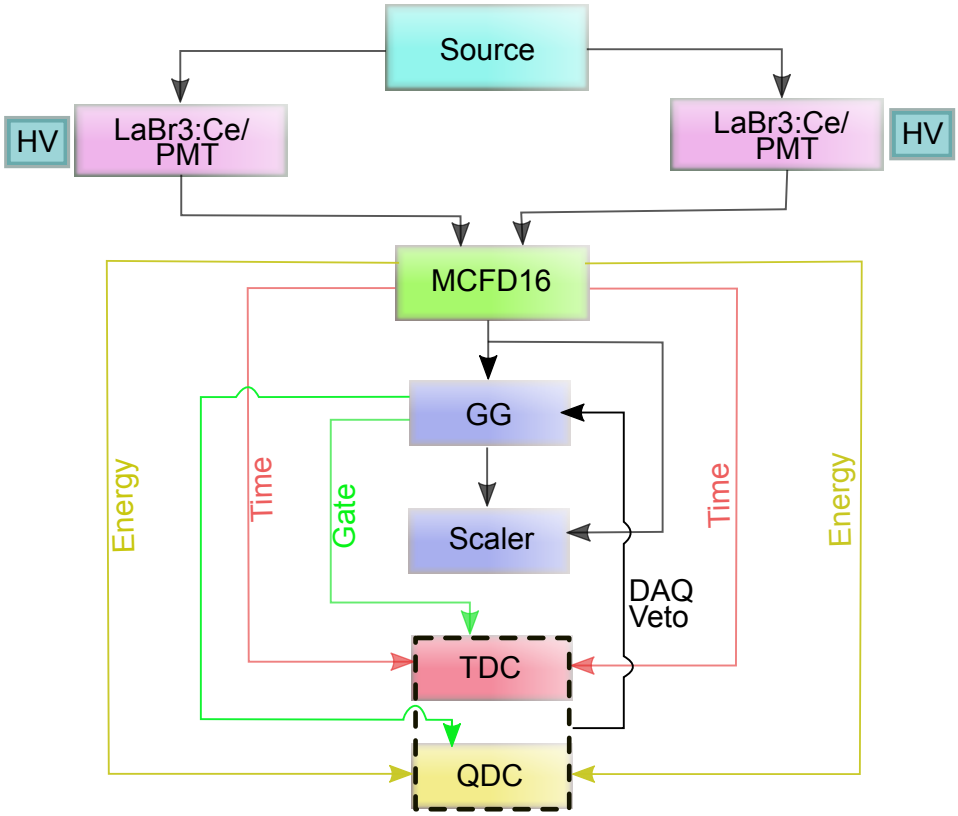

Figure 7: Scheme of the electronic setup for two of the 14 detectors.

The digital signals from the data acquisition and from the scaler are sent to a computer, where the data can be analyzed as a histogram (intensity versus energy) in the Kmax software. The elemental composition can be identified from the histogram, depending on the energies at which the peaks are found and their intensities and the amount can be calculated with the intensity of the peaks. It has to be taken into account that while the system is recording data, there is a loss of data due to the dead time. Dead time is the time period during which the system is busy processing a signal, hence it is not able to process a new event during that time [2].

Chapter 8

8 Experimental Methodology

In this chapter the necessary steps to analyze the samples and identify the elements are explained. First it will be explained how to select the best suited isotopes to analyze, taking into account the neutron activation before the actual measurement. Then it is described how to find a suitable combination of gamma ray coincidences, knowing that every isotope decays in different ways. It is also discussed how some of the isotopes can be detected but others require stronger conditions to be able to measure them.

8.1 Isotopes Selection

The following table shows the trace elements found in the samples and their concentration from the previous studies [7, 8].

Table 1: Elemental concentration. Values from samples (-41,-39,-33) taken from: [8]. Values from samples (-13,+60,+79) taken from: [7].

Depth (cm)	Sample Number	Sc (ppm)	Ni (ppm)	Co (ppm)	Se (ppb)	Sb (ppm)	Th (ppm)
-41	7	3.87 ± 0.2	8 ± 3	4.3 ± 0.02	39 ± 6	0.33 ± 0.05	2.81 ± 0.04
-39	4	8.8 ± 0.1	58 ± 10	16.2 ± 0.1	61 ± 13	1.37 ± 0.14	11.8 ± 0.04
-33	6	1.25 ± 0.02	4.9 ± 1.4	2.97 ± 0.02	1.00 ± 0.001	1.53 ± 0.03	1.95 ± 0.04
-13	5	27.9 ± 0.2	42 ± 4	28.8 ± 0.1	18.6 ± 0.2	1.90 ± 0.08	4.06 ± 0.04
$+60$	3	42.0 ± 0.3	155 ± 6	90.7 ± 0.5	4.54 ± 0.05	0.14 ± 0.08	2.17 ± 0.04
$+79$	8	37.4 ± 0.2	74 ± 5	47.8 ± 0.2	8.4 ± 0.1	0.26 ± 0.08	2.07 ± 0.04

Depth (cm)	Sample Number	Cs (ppm)	Ta (ppm)	Hf (ppm)
-33	6	10.7 ± 0.1	1.92 ± 0.01	2.95 ± 0.01
-13	5	0.284 ± 0.010	3.18 ± 0.02	8.2 ± 0.1
$+60$	3	0.282 ± 0.014	0.282 ± 0.014	6.08 ± 0.1
$+79$	8	0.195 ± 0.013	1.4 ± 0.01	6.34 ± 0.1

It is known that these are some of the elements present in the samples. However, other elements that have not been identified yet could be present in the samples. To be able to detect an element, it has to be taken into account that an element has several isotopes, and when an element is irradiated with neutrons, some of its isotopes can become radioactive, depending on their neutron capture cross section. The neutron capture cross section is a measure of how likely it is for a nucleus to capture the neutron, when a neutron collides with the nucleus. The higher the cross section, the more likely the process is to happen. Every isotope of an

element has a difference abundance, so the neutron capture cross section and abundance must be considered, for example the cobalt isotope ^{59}Co, represents 100% of the abundance of the element (see **Table 2**). By investigating these two characteristics of every isotope it is possible to select which isotope is suited best to be detected in the samples (see **Table 2**).

Table 2: Capture cross section and abundance of the isotopes. Values taken from: [17]

Element	Isotope selected before the NAA	Abundance (%)	Capture cross section (barn)	Reaction occurred
Sc	^{45}Sc	100	27.2 ± 0.2	$^{45}Sc + n \rightarrow {}^{46}Sc$
Cs	^{133}Cs	100	30.3 ± 1.1	$^{133}Cs + n \rightarrow {}^{134}Cs$
Eu	^{151}Eu	47.8	9200 ± 100	$^{151}Eu + n \rightarrow {}^{152}Eu$
Ni	^{58}Ni	68	4.5 ± 0.2	$^{58}Ni + n \rightarrow {}^{58}Co + p$
Co	^{59}Co	100	37.18 ± 0.06	$^{59}Co + n \rightarrow {}^{60}Co$
Se	^{74}Se	0.889	51.8 ± 1.2	$^{74}Se + n \rightarrow {}^{75}Se$
Sb	^{123}Sb	42.787	4.1 ± 0.1	$^{123}Sb + n \rightarrow {}^{124}Sb$
Ta	^{181}Ta	99.988	20.5 ± 0.5	$^{181}Ta + n \rightarrow {}^{182}Ta$
Hf	^{180}Hf	35.0802	13.04 ± 0.07	$^{180}Hf + n \rightarrow {}^{181}Hf$
Th	^{232}Th	98.98	7.35 ± 0.03	$^{232}Th + n \rightarrow {}^{233}Pa$

These samples were activated with thermal neutrons in a reactor for 18 hours with a neutron flux of 2.5x10^{13}neutrons $\cdot$ cm^{-2} $\cdot$ s^{-1}, at the Hoger Onderwijs Reactor in Netherlands [18].

8.2 Gamma ray selection

After identifying which isotopes have a reasonable neutron capture cross section and a good abundance, each isotope has to be studied theoretically by analyzing their gamma ray decay. The gamma rays selected must have a double or triple coincidence to be able to measure the isotope, but at the same time the gamma rays must have high intensities and energies greater than 60 keV, since the spectrometer has a lower resolution for gamma ray energies below that value. In **Table 3** the suitable combinations of gamma rays are shown. For example: ^{60}Co represents a good option to be measured, because it has two very intense gamma ray transitions in coincidences with high energies. The first gamma ray that will be measured has an energy of 1173 keV and goes from the excited state number 3 to 1. There the nucleus stays for 0.00073 ns and then it decays again from state number 1 to the ground state (0) by releasing a second gamma ray with energy of 1332 keV.

Table 3: Gamma rays energies per element used for identification, applying double or triple coincidence conditions. [9]

Isotopes	Decay states	Intensity(%)	Energy (keV)	Time (ns)
^{46}Sc	$\gamma(2,1)Ti$	99.987	1120.54	0.00164
	$\gamma(1,0)Ti$	99.984	889.28	0.0051
^{58}Co	$\gamma(1,0)Fe$	99	810.78	0.00654
	$\gamma(2,1)Fe$	0.683	863.96	0.00126
^{60}Co	$\gamma(1,0)Ni$	99.9856	1332.5	0.000713
	$\gamma(3,1)Ni$	99.9736	1173.24	0.0003
^{75}Se	$\gamma(2,0)As$	58.9	264.66	0.0112
	$\gamma(5,2)As$	58.3	136	1.67
^{124}Sb	$\gamma(1,0)Te$	98.26	602.73	0.0062
	$\gamma(10,1)Te$	47.79	1690.98	———
^{134}Cs	$\gamma(1,0)Ba$	97.62	604.72	0.00512
	$\gamma(3,1)Ba$	85.53	795.86	0,00083
	$\gamma(5,3)Ba$	15.38	569.33	———
^{152}Eu	$\gamma(1,0)Sm$	28.41	121.78	1.4
	$\gamma(13,1)Sm$	20.85	1408.01	———
^{181}Hf	$\gamma(3,0)Ta$	80.5	482.182	10.8
	$\gamma(4,3)Ta$	43.3	133.024	18000
^{182}Ta	$\gamma(7,5)W$	41.2	67.75	1.12
	$\gamma(5,1)W$	34.9	1121.3	0.000434
^{233}Pa	$\gamma(10,7)U$	16.1	75.269	0.0055
	$\gamma(7,1)U$	12.3	300.129	0.052

After having selected the isotope and the coincident gamma ray transitions, the samples can be analyzed. The data acquired from the detection is analyzed with the Kmax software. In the Kmax software energy conditions can be applied to the data. The element identification for the double coincidence is conducted by setting an energy window covering the energy of the high energy gamma ray. The sum energy of the two detected gamma rays is then plotted into a histogram, and the number of detected coincidences for a certain element can be deduced. For example see **Figure 10**.

8.3 Elements measured

Some isotopes could be detected easily by using the double or triple coincidence technique, for example: ^{46}Sc, ^{134}Cs, ^{60}Co and ^{124}Sb. Other isotopes such as: ^{181}Hf, ^{58}Co and ^{152}Eu, were not immediately observed. Some conditions needed to be applied in order to detect them.

8.3.1 Condition applied to measure ^{181}Hf.

Hafnium is one of the isotopes which was not observed directly. A completely pure sample of Hafnium was available in the lab; therefore it was possible to activate it with thermal neutrons. This pure sample was measured for about an hour, and with the data obtained, it could be observed in which time range the double coincidences of the ^{181}Hf occurred more frequently. This time range means the time between the detection of the first gamma ray and the second gamma ray in coincidence. Having this time range, the software Kmax provides a graph that shows the intensity of counts depending on the time difference between the gamma rays (see **Figure 9**). In this graph the desired time range for Hafnium to be selected is from 3.5 ns to 21.3 ns. An additional requirement was that the gamma ray with lower energy must be the first one to be recorded and the opposite applies for the gamma ray with higher energy (see the blue section in **Figure 9**). After applying these conditions in the software is was possible to detect the Hafnium. Also it can be seen in **Table 3** that the time between the two gamma rays in coincidence is 10.8 ns. Therefore, this time is within the requested range from 3.5 ns to 21.3 ns.

8.3.2 Condition applied to measure ^{58}Co.

For the isotope ^{58}Co a condition had to be applied as it was not possible to detect the ^{58}Co immediately due to two reasons. The gamma rays which could be suitable for the coincidence measurement would be a gamma ray from the second to the first excited state and a gamma ray from the first excited to the ground state. However, the second excited state of this isotope is populated by electron capture with the probability of only 1.228%. This percentage is very low, hence it will be a lower probability to observe the isotope. The second reason is that both gamma rays selected have energies which are close to the energies of other elements in the sample, so it is difficult to differentiate them in the graphs. It is known that the ^{58}Co also decays 83.83% by electron capture and 14.94% by positive beta decay to the first excited state (see **Figure 8**). As explained in **Subsection 3.2**, the annihilation process occurs after positive beta decay. Using this information, a condition could be applied in the software that when two detectors in opposite positions (two detectors placed 'back-to-back') captured two gamma rays with energies 511 keV respectively, then there should be a coincidence with an 810 keV gamma ray. This gamma ray corresponds to the decay of the first excited state to the ground state.

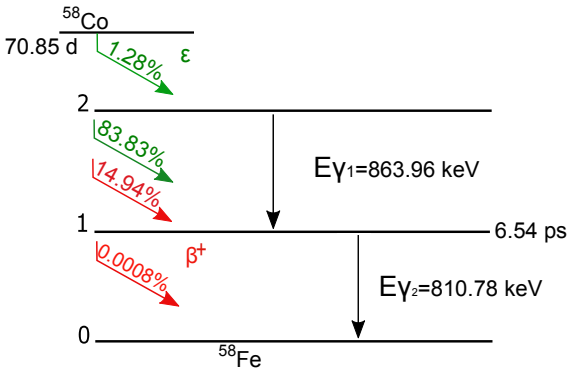

Figure 8: Decay scheme of ^{58}Co. Figure adapted from: [9]

8.3.3 Condition applied to measure ^{152}Eu.

In the analyzed samples it was seen, that the samples have a great amount of another element that was not observed before by the previous studies [7, 8]. This element is Europium. The isotope ^{152}Eu could be seen when the time difference of coincidence was selected between 1.3 ns and 24 ns in the Kmax software. An additional requirement was that the gamma ray with higher energy must be the first one to be recorded and the opposite applies for the gamma ray with lower energy (see the pink range in **Figure 9**).

The **Figure 9** represents the counts as a function of the time difference between the gamma rays in coincidence. For the high-intensity peak, more coincidences were recorded for that specific time difference, as it is shown in the green range of the figure. The right side from 0 ns to 30 ns belongs to the coincidences where gamma rays with the higher energy are captured first and then the gamma rays with lower energy, that is the case of the ^{152}Eu. The left side from 0 ns to -30 ns, where the ^{181}Hf is located, is when the coincidences with low energy gamma ray arrive first to the detector, and then the gamma ray with higher energy.

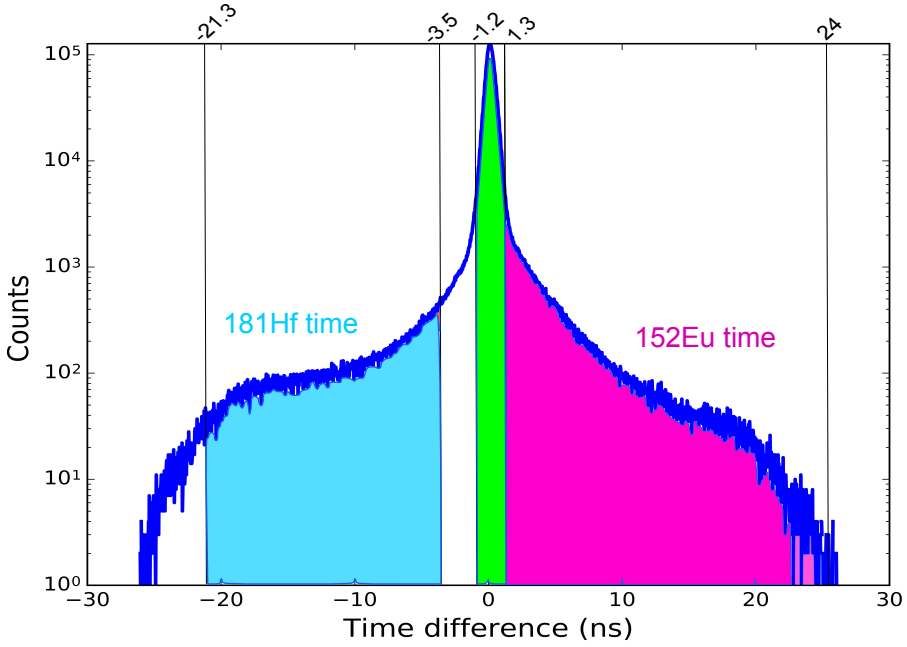

Figure 9: Time difference of coincidence vs counts.

8.4 Compensation and normalization of the counts

The counts provided by the software Kmax are the counts that the spectometer detected during a period of time, but there are some lost counts that must be taken into consideration. Therefore the number of counts obtained for every isotope in each sample were normalized to a standard sample, first by the mass, assuming that the mass of every sample should be 200 mg (see **Table 4**). Secondly the counts were also normalized supposing that they were measured instantly after they were taking out from the reactor. Finally, they were compensated for the dead time.

Table 4: Samples mass

Depth (cm)	Sample Number	Mass (mg)
60	3	120.97
-39	4	187.08
-13	5	195.81
-33	6	67.19
-41	7	128.16
79	8	132.71

Table 4 shows the sample masses and the relation between the sample number and the depth of the ash layers, information taken from: [7,8].

8.5 Minimum Detectable Limit calculation

The detection threshold of a counting system depends on the counts from the background. The National Bureau of Standards established that the Minimum Detectable Activity (MDA) of a counting system is equal to three times the standard deviation of the background count rate.

$$\text{MDA} = 3\gamma\sqrt[2]{\text{n}_b} \tag{8}$$

where γ represents a correction factor to transform the result from counts per minutes to Bq/mg. Becquerel (Bq) is the SI derived unit of radioactivity and n_b is the number of counts from the background per minutes [19].

In this work, however, a similar value to the MDA, the Minimum Detectable Limit (MDL) was calculated. The MDL is the smallest amount in ppm in the sample in order to be able to detect the element in the sample. This value was obtained by multiplying 3 times the square root of the number of counts detected from the background during a period of time of 24 hours. By using the amount of the element in ppm given by [7, 8], the number of counts during 24 hours period and the number of background events N_B in the same time period, the MDL can be calculated.

$$\text{MDL} = \left(\frac{\text{Amount of the element(ppm)}}{\text{number of counts 24 h}}\right) * 3\sqrt[2]{\text{N}_B} \tag{9}$$

Chapter 9

9 Results and Discussion

9.1 Results

Table 5 presents the number of compensated and normalized counts of every isotope measured in the samples, with their uncertainties. The statistical uncertainties are calculated by using the number of counts measured, $\frac{1}{\sqrt{N_c}}$; (N_c=Number of counts). The uncertainties are calculated from the uncompensated number of counts.

Table 5: Compensated counts of every isotope in the samples.

Sample	Counts compensated			
	^{46}Sc	^{58}Co	^{60}Co	^{181}Hf
3	452172±388	1078±18	30835±133	35822±83
4	118930±273	470±17	7136±80	21991±97
5	121447±279	152±10	3934±61	18326±90
6	29930±77	82±4	2432±28	38160±68
7	196087±286	388±12	6985±66	17344±69
8	278022±347	356±12	11580±86	23895±84

Sample	Counts compensated		
	^{124}Sb	^{134}Cs	^{152}Eu
3	225±8	9100±71	15098±94
4	900±22	43637±196	2100±44
5	453±16	2910±51	1596±39
6	1695±17	89156±168	1447±22
7	693±16	34380±145	3921±50
8	124±7	5704±59	3620±48

By using one sample as a reference and knowing the elemental concentration from [7, 8], it was possible to calculate the elemental concentration of the other samples. The reference samples are highlighted in gray in **Table 6**. This means that their number of counts per second detected and the previous measurements of the elemental concentration (in ppm), were used as a reference to calculate the elemental concentration of the other samples.

Table 6: Estimation calculated of the isotopes concentration.

Sample	^{60}Co		^{124}Sb	
	Ref (ppm)	Exp (ppm)	Ref (ppm)	Exp (ppm)
3	90.7±0.5	90.7±0.7	0.14±0.08	0.40±0.05
4	16.2±0.1	19.0±0.2	1.4±0.1	1.46±0.07
5	28.8±0.1	27.1±0.4	1.90±0.08	1.9±0.1
6	2.97±0.02	4.0±0.1	1.53±0.03	1.7±0.1
7	4.30±0.02	4.75±0.07	0.33±0.05	0.29±0.02
8	47.8±0.2	52.0±0.6	0.26±0.08	0.34±0.05

Sample	^{58}Co		^{46}Sc	
	Ref (ppm)	Exp (ppm)	Ref (ppm)	Exp (ppm)
3	155±6	155±9	42.0±0.3	42.0±0.1
4	58±10	61±4	8.8±0.1	9.98±0.04
5	42±4	51±5	27.9±0.2	26.4±0.1
6	4.9±1.4	7±2	1.25±0.02	1.54±0.02
7	8±3	13±1	3.87±0.02	4.21±0.01
8	74±5	78±7	37.4±0.2	39.4±0.1

Sample	^{181}Hf		^{134}Cs	
	Ref (ppm)	Exp (ppm)	Ref (ppm)	Exp (ppm)
3	6.1±0.1	6.83±0.08	0.28±0.01	0.380±0.005
5	8.2±0.1	8.17±0.09	0.28±0.01	0.284±0.006
6	2.95±0.01	4.03±0.06	10.7±0.1	2.06±0.01
8	6.3±0.1	6.95±0.08	0.20±0.01	0.363±0.006

The minimum concentration per isotope needed in a sample, in order to guarantee the presence of the isotope, was calculated using the concentration from the previous measurements [7,8] (see **Table 1**), and the counts from the background. This result is shown in **Table 7**.

To give an estimation of the background, the number of background counts was measured by integrating the counts on the high-energy side of each peak. The selected range is equal to the peak width. See, for example, **Figure 10** where the background range is highlighted in green.

Table 7: Minimum Detectable Limit for the sample 8.

Sample 8	Concentration (ppm)	Compensated Counts for 24 h	Background counts for 24h	Minimum of counts needed	MDL (ppm)
^{46}Sc	37.4±0.2	700630±2014	1759±69	126±2	0.007±0.200
^{134}Cs	0.20±0.01	14375±242	12±7	10±3	0.0001±0.0102
^{60}Co	47.8±0.2	29182±340	44±13	20±3	0.03±0.20
^{58}Co	74±5	897±75	70±21	25±4	2±5
^{124}Sb	0.26±0.08	311±46	97±26	30±4	0.02±0.10
^{181}Hf	6.3±0.1	60216±717	2010±133	135±4	0.01±0.10
^{152}Eu	———	9122±189	47±14	21±3	———

The MDL was calculated using the compensated counts, therefore it represents the MDL of a sample with 200 mg, that was measured directly after being irradiated in the neutron reactor and measured for 24 hours.

The following plots show the peaks obtained for every isotope in sample 4 after performing the analysis with double or triple coincidences. The coincidence conditions applied for each isotope are seen in **Table 3**. The graphs show the number of counts versus the sum of energies of the two or three gamma rays in coincidence. The pink areas represent the energy range used to identify the elements. The energy range selected for every isotope is the range around the peak. As it can be seen in the figures, most of the plots have been cut in the software below an approximate energy of 1200 keV, which is done for better visibility.

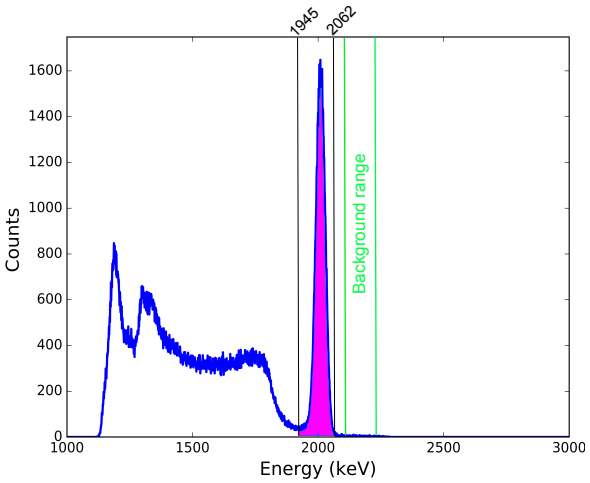

Figure 10: Energy spectrum of ^{46}Sc. Sum of double coincidence energies: 1120.54 keV and 889.28 keV.

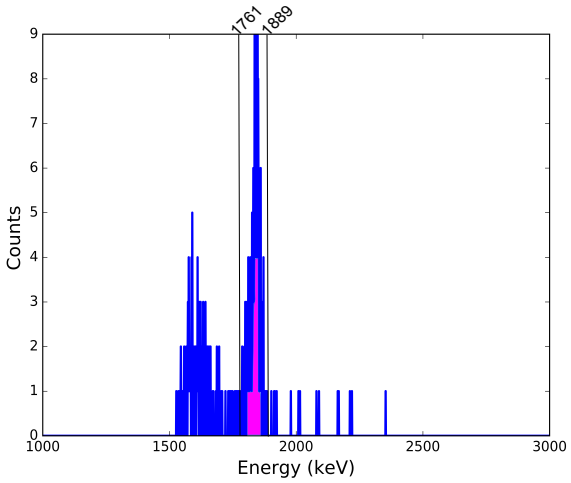

Figure 11: Energy spectrum of ^{58}Co. Sum of double coincidence energies: 810.78 keV and 863.96 keV.

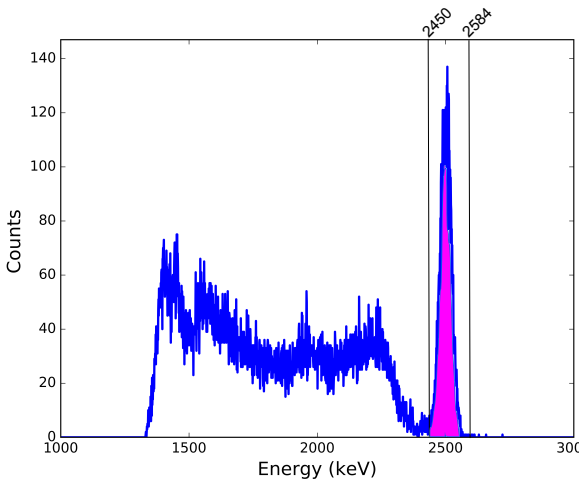

Figure 12: Energy spectrum of ^{60}Co. Sum of double coincidence energies: 1332.5 keV and 1173.24 keV.

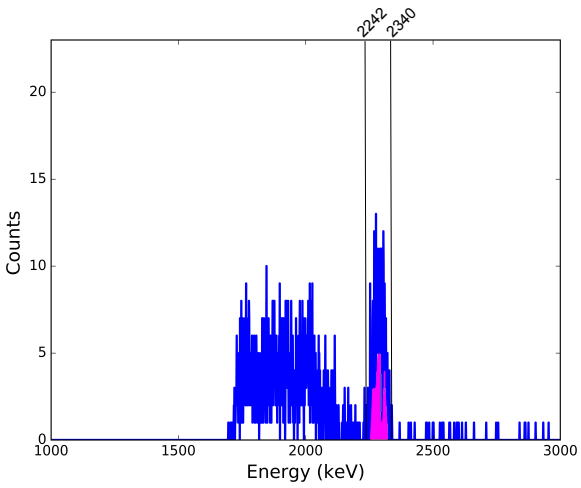

Figure 13: Energy spectrum of ^{124}Sb. Sum of double coincidence energies: 602.73 keV and 1690.98 keV.

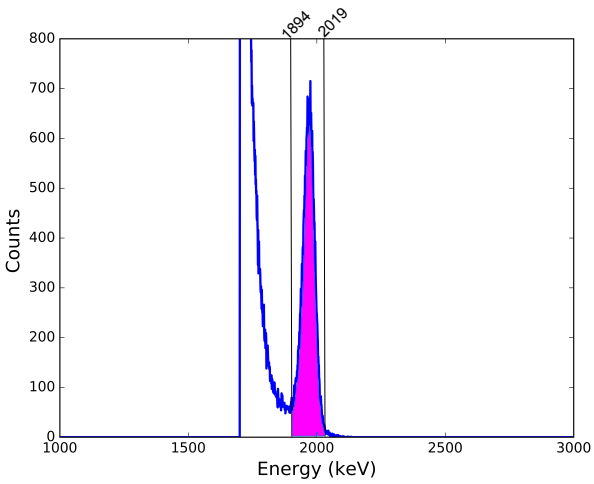

Figure 14: Energy spectrum of ^{134}Cs. Sum of triple coincidence energies: 604.72 keV, 795.85 keV and 569.33 keV.

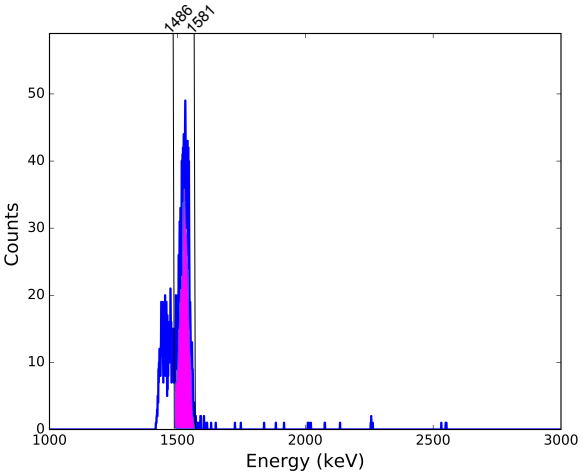

Figure 15: Energy spectrum of ^{152}Eu. Sum of double coincidence energies: 121.78 keV and 1408.01 keV.

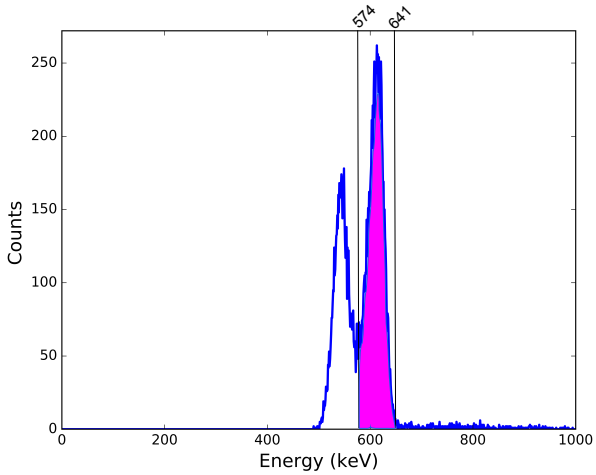

Figure 16: Energy spectrum of ^{181}Hf. Sum of double coincidence energies: 482.182 keV and 133.024 keV.

9.2 Discussion

The trace element analysis based on the neutron activation, using the 14 $LaBr_3$:Ce detectors spectrometer in coincidence mode, represents a good and non destructive element analysis technique. The method does not only allow identification of an element, but it can also detect the element even if the amount in the sample is on the order of ppm or below. This advantage is demonstrated in **Table 7**.

The experiment allowed to detect 7 elements from the samples, 6 of them were already expected to be in the samples from previous studies [7, 8], these are: ^{46}Sc, ^{134}Cs, ^{60}Co, ^{58}Co, ^{124}Sb and ^{181}Hf. The seventh isotope identified in the samples is ^{152}Eu. Additionally, ^{182}Ta and ^{233}Pa were also expected to be found. However they could not be detected because the best suitable combinations of the gamma rays were with very low energies (see **Table 3**). In the case of ^{182}Ta, the gamma ray which should have been detected follows the decay $^{182}Ta \rightarrow \gamma(7,5)W$ and it has an energy of 67 keV. In the case of ^{233}Pa, the gamma ray sought before is from the following decay $^{233}Pa \rightarrow \gamma(10,7)U$ and it has a energy of 75 keV. These low energies make it hard to distinguish the elements from the large Compton background.

Using the knowledge from previous studies [7,8], it was possible to calculate the elemental concentration in each sample (see **Table 6**). Most of the results were in good agreement, but for some elements the measured value and the reference value does not agree. This might be explained by sample heterogeneity and the fact that the samples analyzed are prepared from the same collected sample material, but not from the same sample, so they do not have the same distribution of the elements.

The clear and intense peaks obtained in the plots are thanks to the combination of: the high resolution supplied by the detectors, the appropriate detector setup, that surrounded almost all the source radiation and the use of double and triple coincidence conditions. Without these conditions satisfied, the spectra would have been full of background from Compton scattering.

In conclusion it was possible to identify more trace elements from the ash samples by using the coincidence spectrometer. The 14 $LaBr_3$:Ce detectors coincidence spectrometer is an appropriate technique for the detection and analysis of the trace elements. It gives to the experimenter a clean spectrum with intense peaks, suppressing the background. This rapid and

non-destructive measurement technique represents a good tool for detection and calculation of very small amounts of elements, in different research areas such as the geological area.

10 References

References

[1] Krane K. Introductory nuclear physics. 1st ed. New York: John Wiley and Sons; 2005.

[2] Knoll G. Radiation detection and measurement. 4th ed. New York: Wiley; 1979.

[3] Crouthamel C, Adams F. Applied gamma-ray spectrometry. 1st ed. Oxford: Pergamon; 1975.

[4] Bonolis L. Walther Bothe and Bruno Rossi: The birth and development of coincidence methods in cosmic-ray physics. American Journal of Physics; 2011.

[5] Oshima M, Toh Y, Hatsukawa Y, Hayakawa Y, Shionohara N. A High-sensitivity and Non-destructive Trace Element Analysis Based on Multiple Gamma-ray Detection. Journal of Nuclear Science and Technology. 2002;39(4):292-294.

[6] Vertes A. Handbook of nuclear chemistry. 1st ed. Dordrecht: Springer; 2011.

[7] Schmitz B, Lindström M, Asaro F, Tassinari M. Geochemistry of meteorite-rich marine limestone strata and fossil meteorites from the lower Ordovician at Kinnekulle, Sweden. Earth and Planetary Science Letters. 1996;145(1-4):31-48.

[8] Schmitz B,Asaro F. Iridium geochemistry of volcanic ash layers from the early Eocene rifting of the northeastern North Atlantic and some other Phanerozoic events. Geological Society of America Bulletin. 1996;108(4):489-504.

[9] Nucleide-Lara on the web (2017) [Internet]. Nucleide.org. 2017 [cited 26 April 2017]. Available from: http://www.nucleide.org/Laraweb/

[10] Leo W. Techniques for nuclear and particle physics experiments. 2nd ed. Berlin: Springer-Verlag; 1994.

[11] Aymen H. Study of Gamma-ray Response of LaBr3:Ce Scintillation Detectors for an Iridium Coincidence Spectrometer.[Master]. University of Lund, Department of Physics; 2012.

[12] Oliver Roberts, P. J. Neutron response of 1.5 LaBr3:Ce crystal scintillators for PARIS. Heslington,YO10DD,UK: University of York, Department of physics; 2008.

[13] V792N 16 Channel Multievent QDC. CAEN, Electronic Instrumentation; 2016.

[14] V1290N 16 Channel Multievent TDC. CAEN, Electronic Instrumentation; 2017.

[15] MCFD-16, 16 channel CFD with fast amplifier and pattern processing. Putzbrunn, Germany; 2008.

[16] Sparrow, Kmax - Advanced Tools for Industry, Education and Research [Internet]. Sparrowcorp.com. 2017 [cited 4 April 2017]. Available from: http://www.sparrowcorp.com/products/software

[17] Mughabghab S.F. Thermal neutron capture cross sections resonance integrals and G-Factors. Brookhaven National Laboratory, US Department of Energy; 2003.

[18] Blaauw M. Hoger Onderwijs Reactor (HOR) [Internet]. Delft University of Technology. 2017 [cited 4 May 2017]. Available from: http://www.tnw.tudelft.nl/en/cooperation/facilities/reactor-instituut-delft/research/facilities/hoger-onderwijs-reactor-hor/

[19] Radiation Counting Statistics [Internet]. 2017 [cited 4 April 2017]. Available from: http://holbert.faculty.asu.edu/eee460/RadiationCountingStatistics.pdf

.